Kinetic Control of High-Pressure Solid-State Phase Transitions: A Case Study on L-Serine

Martin Fisch, [a,b] *Arianna Lanza,* [a,b] *Elena Boldyreva,* [c,d] *Piero Macchi,* [*,a] *and Nicola Casati* [*,b]

[a]Department of Chemistry and Biochemistry, University of Bern,

Freiestrasse 3, 3012 Bern, Switzerland

[b]Synchrotron Radiation and Nanotechnology, Swiss Light Source,

Paul Scherrer Institute, 5232 Villigen, Switzerland

[c]Institute of Solid State Chemistry and Mechanochemistry,

Russian Academy of Sciences, Siberian Branch, Russia

[d]Novosibirsk State University, Russia

AUTHOR INFORMATION

Corresponding Author

*Email: piero.macchi@dcb.unibe.ch, Tel: +41 31 631 42 81

*Email: nicola.casati@psi.ch, Tel: + 41 56 310 53 46

Abstract

This study demonstrates that the compression rate adds a new perspective to phase diagrams of solids. A particular pressure increase rate may trigger unexpected solid-state transformations, producing otherwise inaccessible phases. Our test case is L-Serine, characterized by a complex high-pressure behavior with three known polymorphs. However, the critical pressure of each transition, the ranges of co-existence of polymorphs, and the existence of an elusive fourth phase remained open questions, here analyzed and solved using synchrotron powder X-ray diffraction at high pressure, under controlled pressure increase rates. Two parallel paths exist and the composition of the system depends on the pressure increase rate and the steps during the compression. A slow and continuous compression favors phase IV, whereas phase II can be observed only with a rapid and sharp compression. No direct inter-conversion occurs between these phases. Moreover, phase III originates only from phase II, but never from phase IV. By controlling the strategy of pressure increase, we obtained a powder of phase IV that enabled solving its unknown structure, which resulted as a distorted superstructure of phase I with a tripled *a*-axis.

Introduction

Applying pressure (P) is a method to change the thermodynamic state of a material. Depending on the pressure range, the energy transferred to the system is capable of altering the electronic structures of atoms or molecules and, consequently, the positions of atomic nuclei. This can result in lattice strain, structural changes (phase transitions) or even chemical reactions. The complexity of the potential energy surface of a crystalline material implies that one should consider the deep entanglement of thermodynamic and kinetic factors, which may affect transformation paths and the final products.

While reversible processes are usually implicitly assumed, more often non-equilibrium transformations occur, meaning that the system does not follow a thermodynamic path. This holds true when a crystal is over-cooled or over-heated or otherwise rapidly compressed or decompressed. Kinetic effects on temperature variations are often reported since temperature control in an experiment is usually straightforward to achieve. Instead, kinetic effects in P-induced transformations are less predictable and the occurrence of metastable phases is often not recognized. Hints of kinetically controlled phenomena are, for example, non-equivalent transformations of single-crystal and powder samples, coexistence of multiple phases over extended pressure ranges and occurrence of different forms depending on the time a sample is kept at a selected pressure.[1] Noteworthy, during high-pressure (HP) experiments, the rate of the compression is extremely important, but it is often not controlled. A temperature gradient of 100 K/h or a pressure increase rate of 10 GPa/h are equally possible with standard instrumentation. However, while the former is not dramatic for a solid-state sample, the latter can be rather effective and significantly alter the results of a pressure scan. Recent developments in analytical methods allow for extremely fast HP experiments, with even higher compressing rates, and dynamic time-

resolved investigations at HP have become of high interest.[1–3] For example, modified diamond anvil cells (DACs), such as the dynamic DAC (dDAC), allow repetitive loadings with rates up to 500 GPa/h.[4–9] Computer-controlled membrane DACs can be used over larger pressure ranges and offer the possibility of rate-dependent compression and decompression.[10,11]

We have become interested in these phenomena while studying pressure induced phase transitions in magnetic coordination polymers,[12] and decided to investigate in more detail how the pressure increase rate (PIR) may affect transformations, focusing on simple molecular crystals.

The samples most affected by non-equilibrium transformations are soft materials, assembled through weaker intermolecular interactions, such as most molecular crystals. Hydrogen bonds in extended networks can act as springs and molecular fragments as joints and hinges, accounting for various structural rearrangements. Sometimes the new phases, generated by these rearrangements, may compete at the same pressure and even subtler modifications of the experimental conditions may favor one or another.

Within soft organic crystals, a very well-studied class is that of amino acids, due to the matchless interest in studying properties of the molecules at hearth of bio-systems (the so-called biomimetic) and to the growing interest in amino acids as building blocks of materials with e.g. nonlinear optical, piezoelectric and ferroelectric properties.[13] Many recent studies have dealt with compressed amino acid solids to gain insight into the role of intermolecular interactions on phase changes at HP.[1,13–19] However, time and PIR have only recently been addressed as crucial factors.[20] The stereochemical flexibility of some of these molecules may easily produce kinetically stable intermediates and indefinitely preserved metastable phases. While the free energies of various polymorphs are typically very close, their interconversion may be associated with high energy barriers that include nucleation and nuclei growth. The barriers of each of these stages can be very

different and have different dependences on pressure. In particular, the probability of nucleation may also depend on the compression rate, as analogously proposed for temperature gradients.[21]

In this study, we focus on L-Serine (L-Ser, $^{+}(NH_3)$-$CH(CH_2OH)$-COO^{-}), known for its rich HP polymorphism. Several studies[22–25] have characterized the structures of L-Ser II (observed above 5.4 GPa) and L-Ser III (observed at ca. 8.0 GPa) from single-crystal X-ray diffraction (XRD). Synchrotron diffraction experiments on powders[25] have shown coexistence of L-Ser I and II up to 6.3 GPa and peaks of an unknown fourth polymorph above 6.4 GPa. On the other hand, in powder neutron diffraction experiments, neither phase coexistence nor unindexed peaks were reported.[26,27] Noteworthy, experiments were carried out with different anvil cells, different control of the pressure increase and different compression steps.

Having this complicated puzzle in mind, we decided to carefully investigate all the phase transitions maintaining an accurate control not only of the pressure but also of the PIR. After rationalizing the conditions that govern the transition paths (Fig. 1), we could obtain a rather abundant amount of L-Ser IV in powder, from which we solved its so-far unknown structure. Periodic density functional theory was used for optimizing the crystal geometries of the solutions from simulated annealing and therefore determining more accurate positions of H atoms.

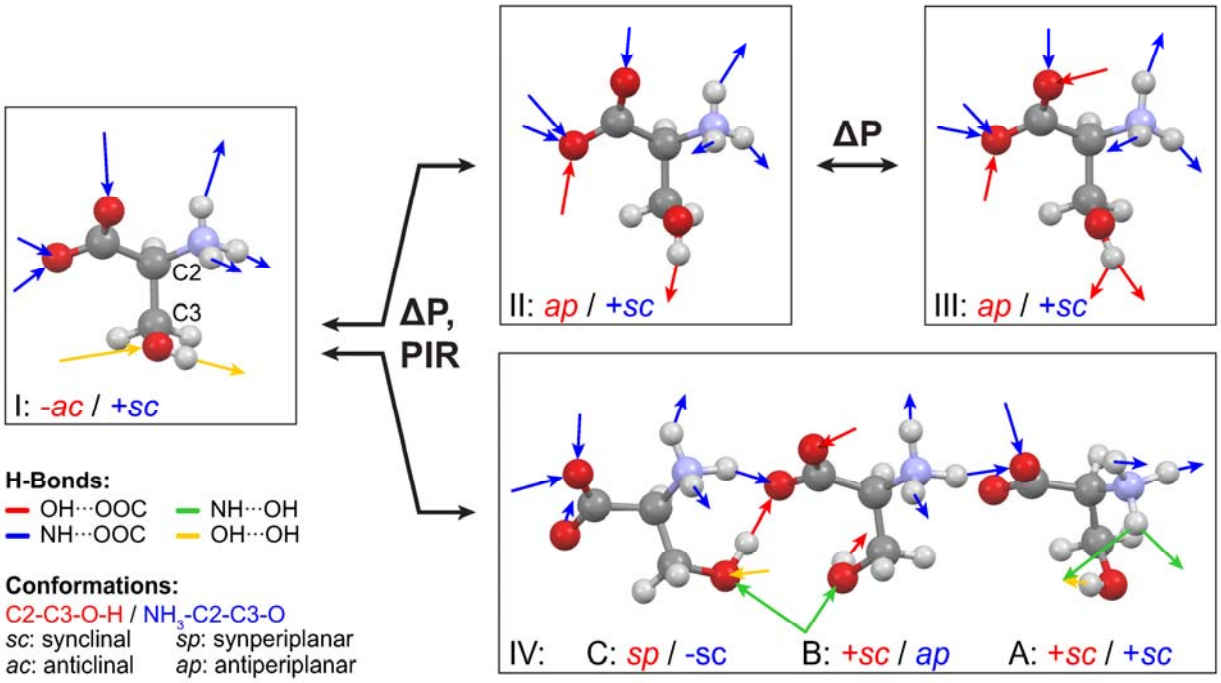

Figure 1. The H-bond sites and conformational changes in L-Serine at HP. L-Ser I transforms to L-Ser II and/or IV at HP, depending on the compression protocol. II subsequently transforms to III at higher pressure whereas IV remains stable up to at least 9.5 GPa.

Experimental Methods

We define the PIR as the ratio between a given pressure step (in GPa) and the time required for (A) reaching target pressure, (B) sample equilibration and (C) rapidly collecting diffraction data. A typical measurement consists of several consecutive cycles, ideally all at the same PIR, up to the maximum pressure (Fig. S4). Maintaining a constant PIR requires a precisely controllable DAC and rapid manipulation to increase the pressure. The elective instrument is a remotely controlled gas membrane DAC. The PIR cannot be regulated with a direct feedback of the internal pressure, but only after determining a precise correlation between the directly controlled gas pressure in the membrane and the pressure inside the DAC (Fig. S5). Remote control of the DAC was realized by

extending the pressure line between the DAC on the diffractometer and the manually controlled gas controller in the control room to a length of about 10 m.

Certified TraceCERT® L-Serine reference material was used throughout all experiments (Sigma Aldrich 54763-100MG, Lot# BCBH42640V). The sample was hand-ground in an agate mortar. Pressure medium in all runs was a 4:1 mixture of MeOH:EtOH to ensure hydrostatic conditions to above 9.5 GPa.[28]

Three different PIR dependent HP experiments and two runs, in which the pressure was raised with a given PIR and subsequently held while repeatedly measuring the sample were performed (Table 1). Data for the structure solution of L-Ser IV were obtained from a sample loaded into a screw-driven Merrill-Basset DAC. The membrane DAC used for the PIR dependent experiments was equipped with 0.5 mm diamond anvils and steel gaskets preindented to about 70 to 90 μm with a hole diameter of 0.2 mm were used. Pressure was determined from lattice parameters of admixed quartz[29] in the 5 GPa/h run. Data for the structure solution of L-Ser IV were obtained from a sample loaded into a screw-driven Merrill-Basset DAC equipped with 0.6 mm culets. The steel gasket with a hole of 0.25 mm was preindented to about 90 μm. Pressure was raised with steps ≤ 0.56(6) GPa, while keeping the PIR below 1 GPa/h, to a value of 6.64(6) GPa, as determined from ruby fluorescence.[30]

Powder XRD experiments were performed at the X04SA Materials Science beamline[31] at the Swiss Light Source, Paul Scherrer Institute. The diffractometer is equipped with a Mythen II detector, which can provide fast data collection speed. Patterns from -40 to +40 ° in 2θ were collected with a typical time of 1 minute. Radiation was monochromated to 16 keV and attenuated using a 0.8 mm Si filter. The focused primary beam was slitted to about 100 by 100 μm^2.

Diffraction data were treated with TOPAS Academic V5.[32] For the 5 GPa/h dataset, Le Bail refined lattice parameters of each L-Serine polymorph were parameterized[33] to an equation of state. Once they are known (Table S1), pressure can be directly determined from L-Serine lattice parameters (Table S2, Figs. S1, S2, S3). Site coordinates for Rietveld quantification (Figs. S7 and S8) were taken from literature (L-Ser I: CCDC 249277;[22] L-Ser II: CCDC 889408;[19] L-Ser III: CCDC 624342[26]). Peaks of the new L-Ser IV could be indexed from a dataset at 6.64(6) GPa in space group $P2_12_12_1$ with a = 16.09873(5), b = 8.42773(2) Å, c = 8.04459(7), V = 1091.46(2) Å^3. Starting from a threefold superstructure of L-Ser I, the structure of L-Ser IV was solved by simulated annealing.[34] The preliminary structure solution was used as starting model for periodic DFT calculations using full electron 6-31G(d,p) basis set with CRYSTAL09.[35] The final structure (R_{Bragg} = 10.2 %, Fig. S9, Tables S3 and S4, CCDC 1412832) was repeatedly obtained in simulated annealing runs by using molecular geometries from the converged DFT calculation.

The topological analysis of hydrogen bonds was performed with ToposPro V5.0.1.0.[36] The H-bond network was obtained by selecting D-H···A interactions simultaneously fulfilling the requirements: H···A ≤ 2.5 Å, D···A ≤ 3.5 Å and DHA angle ≥ 120°. The underlying net for all L-Serine polymorphs (Fig. 2) was obtained by applying the standard simplification method with the ADS module. The simplified molecular skeletons (Fig. 3) were obtained by selecting the Cα carbon as central atom and replacing the three main functional groups with a single "atom" at the position of their center of mass.

Table 1. Overview of HP data collections on L-Serine.

Run	GPa/h	Steps/GPa	min/Step	P_{Max} [GPa]
1 GPa/h	1	3	20	9.32(2)
5 GPa/h	5	4	3	9.46(2)
10 GPa/h	10	2	3	9.39(2)
Held at 5.5	5	n/a	19 x 5 + 17 x 30	5.50(2)
Held at 6.3	1	n/a	4 x 6 + 13 x 30	6.30(2)
L-Ser IV	< 1	≥ 2	> 30	6.64(6)

Results

Crystal structures. At ambient conditions, the molecules in L-Ser I are linked through a 3D hydrogen bond network. The $–NH_3$ and –COO groups form robust head-to-tail chains via NH···O hydrogen bonds, which are additionally stabilized by OH···OH hydrogen bonds between the side $–CH_2OH$ groups of the neighboring chains (Fig. 1-I). At HP, the side chains rotate to form –OH···O=C– hydrogen bonds with the –COO groups in L-Ser II (Fig. 1-II) and subsequently additional bifurcated NH···O hydrogen bonds in L-Ser III (Fig. 1-III). Table 2 summarizes the main intermolecular connections of the different species.

With respect to the previously known HP phase II, L-Ser IV provides an alternative way to reduce the molar volume of phase I. As in the L-Ser I → II transition, the side chains rotate, but only two out of three OH···OH bonds break in favor of OH···OOC interactions, resulting in a tripling of the *a*-axis (Fig. 1-IV). In particular, the hydroxyl group, which has an anticlinal (-) conformation in L-Ser I, is synperiplanar, synclinal (+) and synclinal (+) in the three symmetry independent molecules of L-Ser IV, respectively. The conformations of –OH also affect the $–NH_3$ groups. New NH···OH interactions result from the torsion of one of the three $–NH_3$ groups. The conversion of L-Ser I into IV increases the number of short intermolecular interactions per molecule, in keeping with the higher density of this structure. While in L-Ser I, each molecule forms eight H-bonds with eight different neighboring molecules, two thirds of the molecules are

participating in nine H-bonds in L-Ser IV. This arrangement also differs from that of L-Ser III, which has ten hydrogen bonds per molecule. In L-Ser IV, pairs of adjacent molecules are connected by one or two H-bonds, while, in all other known polymorphs, pairs of neighboring molecules are connected by only one H-bond. Although L-Ser II is always denser than I (and even denser than IV) at each pressure point in the investigated range, it is still assembled through only one hydrogen bond per pair of molecules.

The underlying net,[36] representing each molecule as a node and each H-bond as an edge (Fig. 2) is a way to reduce the structural information and appreciate similarities and differences among the phases. L-Ser I is a uninodal 8-connected net, corresponding to the **hex** topological type.[37] L-Ser II corresponds to the same underlying net, the only difference lying in the type of interaction (OH···OH vs. OH···OOC, as shown in Fig. 2). For L-Ser III, instead, the uninodal underlying net is 10-connected, corresponding to the **tcg** topological type.[38] By applying the same criteria, L-Ser IV can be described as a 2-nodal net, where the nodes (corresponding to three crystallographically independent molecules) have coordination number 7, 6 and 7 respectively, corresponding to an unprecedented topological type.

Table 2. The main H-bonding interactions in all L-Serine polymorphs: on the left side I is compared with II and III, on the right a superstructure of I is compared with IV.

I		II		III		Polymorph		I (Superstructure)						IV					
						Interaction		a		b		c		a		b		c	
D	A	D	A	D	A	Donor (D)	Acceptor (A)	D	A	D	A	D	A	D	A	D	A	D	A
3	3	3	3	3	3	NH	COO	3	3	3	3	3	3	2	3	3	2	3	3
1	1					OH	OH	1	1	1	1	1	1	1					1
		1	1	2	2	OH	COO									1	2	1	
						NH	OH							2			1		1
8		8		10		Intermolecular HBs		8		8		8		8		9		9	
8		8		10		H-bonded molecules		8		8		8		7		6		7	
hex		hex		tcg		Underlying net		hex						New binodal 7,6,7-c net					

The correlation between L-Ser IV and I is better visualized using an intermediate degree of simplification (Fig. 3): each molecule is represented by the three main functional groups conjoined at the Cα. In this way, it appears more evident that the L-Ser IV H-bond network contains motifs already present in the network of L-Ser I with different extent of deformation and is completed by additional bonds.

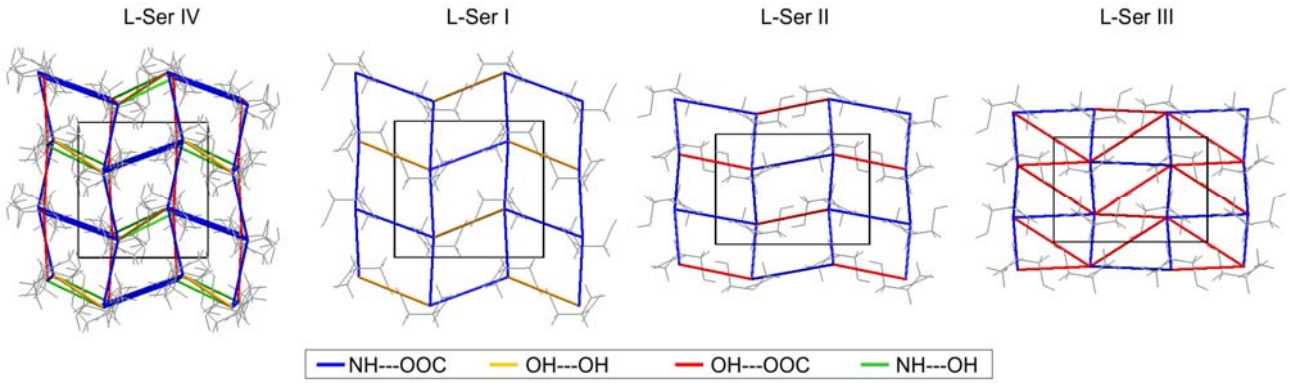

Figure 2. The nets produced by polymorphs I, II, III and IV constructed with each molecule as a node and each H-bond as an edge. Viewed along *a*.

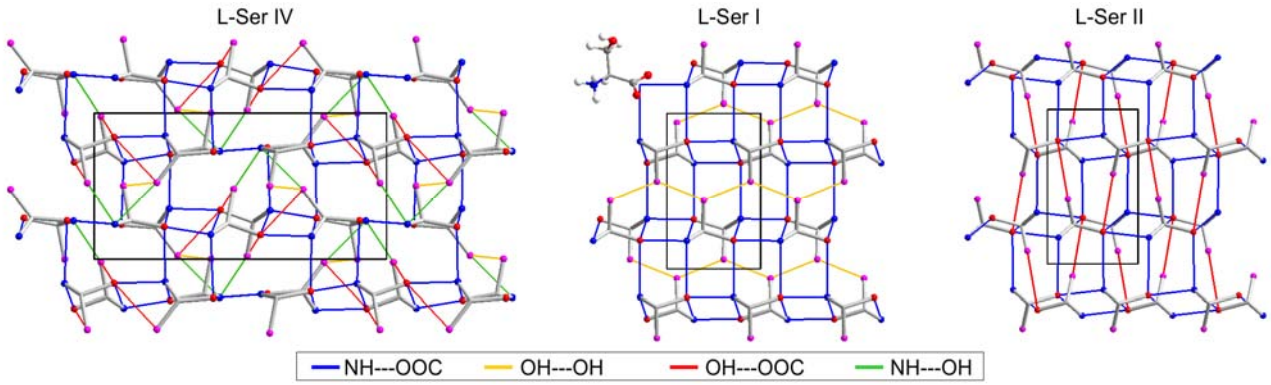

Figure 3. The nets produced by polymorphs I, II and IV. Each molecule is simplified by a skeleton representing the three main functional groups. Viewed along *b*.

Sample composition. The volume per molecule vs. pressure and relative phase occurrences are plotted in Fig. 4 for each PIR (enlarged in Fig. S1). Figures S2-S3 and Tables S1-S2 contain additional information..

In our experiments, the pressure range, in which L-Ser I is identified extends from room pressure up to 8.80(2) GPa, which is a significantly larger range than so far reported (i.e. 0–6.3 GPa[25]). In contrast, onset of L-Ser II occurs between 5.17(2) and 5.43(2) GPa and L-Ser III between 8.02(2) and 8.27(2) GPa as previously reported.[19,23–27] The new phase L-Ser IV is first observed at 5.71(2) GPa, i.e. 0.7 GPa lower than previously reported,[25] and remains stable up to the highest pressure reached in our experiments. After decompression, all HP polymorphs transform back to L-Ser I.

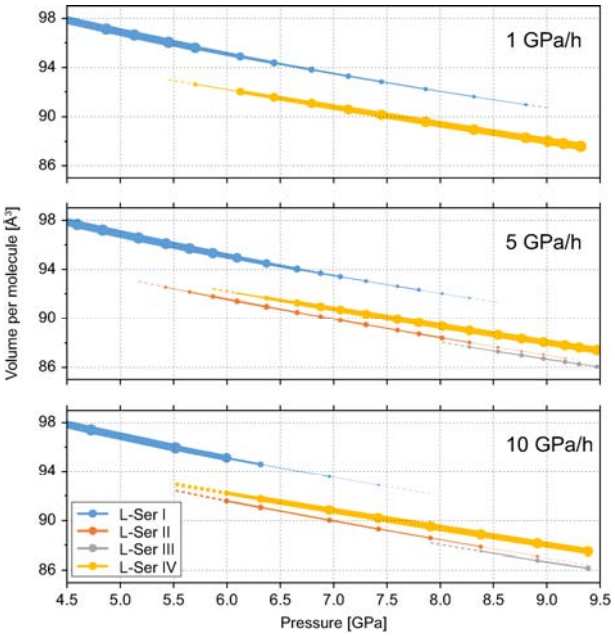

Figure 4. Molecular volume vs. pressure of the three PIR dependent experiments. Phase abundance is proportional to symbol size and line thickness. For each phase, dashed lines indicate the extrapolation to zero amount.

From Fig. 4, it is evident that the range of coexistence depends on the PIR. Interestingly, with PIR = 5 GPa/h all four polymorphs were unambiguously identified at 8.27(2) GPa (Fig. 5). A high PIR accelerates the transformation of L-Ser I, which is completed below 8 GPa at PIR=10 GPa/h whereas it is still observed at 8.80(2) GPa with PIR=1 GPa/h. This is extremely surprising, because one normally expects that a faster compression results in a larger range of metastability of the parent phase. Equally important is the fact that with PIR = 1 GPa/h L-Ser II does not appear and phase III is not formed. This unambiguously demonstrates that L-Ser III can only form from L-Ser II.

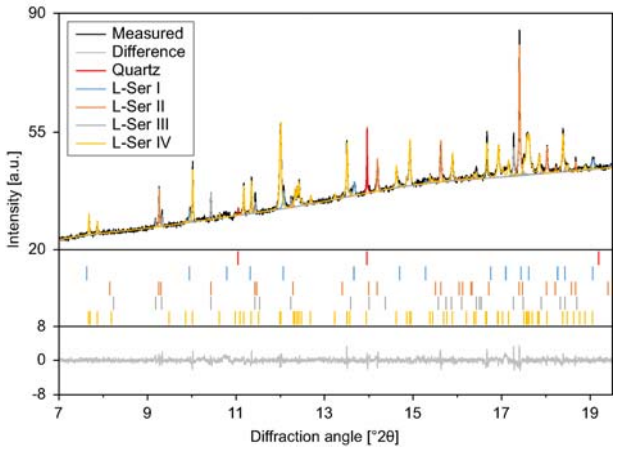

Figure 5. Le Bail refinement of all four L-Serine polymorphs observed simultaneously at 8.27(2) GPa using PIR = 5 GPa/h.

In Fig. 6, we report the semi-quantitative Rietveld results of volumetric composition as function of time for each PIR isochronal experiment (therefore time is linearly proportional to pressure). This shows that, if it forms, phase II reaches a significant volume at a pressure below the onset of IV. However, with PIR = 1 GPa/h, no trace of II is observed and only IV forms, without changing its pressure onset. This observation was very important to prepare a sample consisting mainly of

L-Ser IV at 6.64(6) GPa, thus useful for solving the structure. The occurrence of small traces of phase II inspired another set of experiments: isochronal up to a given pressure, then maintained for long time (8–9 hours). With PIR = 1 GPa/h up to 6.30(2) GPa (Fig. 6), L-Ser IV is observed starting from 5.82(2) GPa, in keeping with the previous 1 GPa/h run. However, after interrupting the compression, a small volume fraction of L-Ser II is quantified (ca. 6 %). Afterwards, L-Ser IV still increases, whereas L-Ser II remains constant. The transformation is however not complete, because ca. 20 % of L-Ser I remains. With PIR = 5 GPa/h up to 5.50(2) GPa (Fig. 6), L-Ser II is first observed, again as in the isochronal experiment, whereas L-Ser IV is observed three minutes later but without further increase of the pressure. L-Ser II and IV continue to form with a rather constant ratio of 1:3 without reaching a stationary state within 8 hours of the experiment. This indicates that the overall rate of formation at this pressure is extremely low for both II and IV. Above this pressure accumulation of IV is always faster whereas II is almost prevented from growing.

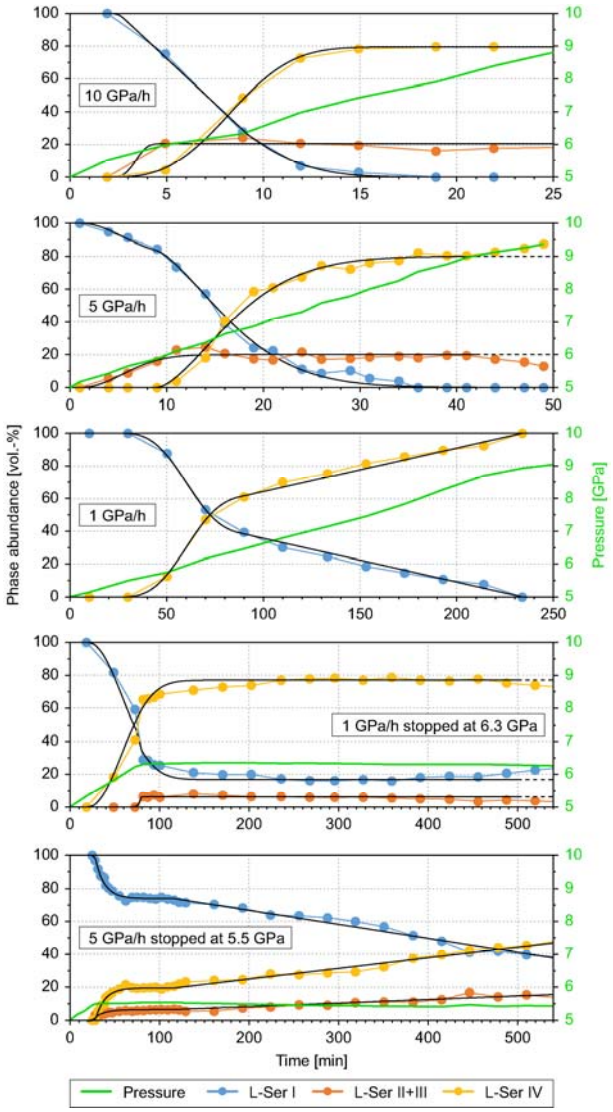

Figure 6. Volumetric phase abundance of L-Serine polymorphs vs. time and pressure for different PIRs. The black lines serve as guide for the eye. Noteworthy for the isochronal experiments (top three graphs), the applied time scale allows a direct comparison as function of the pressure.

Discussion

This study demonstrates the enormous importance of the compression path in typical HP experiments on solids. Measurements carried out using different PIRs on L-Serine show that the compression rate may increase the probability of nucleation of a new phase and its growth rate or otherwise inhibit its formation, eventually modifying the composition of the sample.

We can analyze the observations in terms of pressure and of PIR:

a) Pressure: L-Ser IV is never observed below 5.4 GPa. It cannot be established from these experiments, whether the reason is thermodynamic (IV being still less stable than I in this pressure range) or kinetic. On the other hand, L-Ser II basically stops forming (or it is strongly inhibited) above 6 GPa, whereas transformation of I into IV is observed up to 8.8 GPa. L-Ser III can form only from L-Ser II above 8 GPa, therefore there are two, independent, thermodynamic paths above 6 GPa.
b) Pressure increase rate: a rapid compression enables formation of phase II, at least within the pressure range defined above. Instead, a slow compression hampers the formation of L-Ser II. It is therefore obvious that PIR affects the probability of nucleation of the phases and not only the ranges of metastability of phase I. In particular, a high PIR accelerates the consumption of phase I, therefore reducing the hysteresis, at variance from what normally expected if the PIR would not affect the kinetic of the transformation.

Previous HP single-crystal XRD experiments have never produced L-Ser IV[23,24] and HP powder diffraction experiments[25–27] have shown II as dominant phase. These results are only apparently in contradiction with the above conclusions. In fact, in single-crystal experiments it is sensible to assume that the first phase which nucleates will transform the entire crystal. Because single-crystal experiments are mostly performed with screw-driven DACs, the control on the compression rate

can be much poorer and the actually applied PIR rather high. In the synchrotron powder experiments, Boldyreva *et al.*[25] measured a step at 5.3 GPa, a pressure at which phase IV is still hampered. During the experiment, the system remained at this pressure enough time to produce a rather large amount of phase II, whereas only upon further compression phase IV could form, from the residual amount of L-Ser I and was therefore the minor product. This confirms that below 5.5 GPa, L-Ser IV does not reach significant volume to be seen in diffraction. Moggach *et al.*[26], instead, carried out a neutron experiment at 5.2 GPa, and the sample was maintained at this pressure for long time. Therefore, only phase II was eventually observed.

Conclusions

In this study, we have carefully examined the kinetic control in solid-state transformations of L-Serine at HP. We have clearly demonstrated that the occurrence of the phase most commonly observed above 5 GPa, L-Ser II, is actually due to a particularly high compression rate. As this study has enabled us to define the ideal conditions to prepare preferentially L-Ser IV, we could collect good powder XRD patterns of this phase and solve its so far unknown structure.

The series of experiments reported in this paper and in the previous literature differ in many details such as particle size, amount of material loaded, radiation type and exposure, etc. Nevertheless, all of them confirm the major conclusions drawn in the current study that the formation of L-Ser II and L-Ser IV mainly depends on how rapidly the material is compressed and at which pressure the compression is interrupted for the measurement.

The PIR therefore seems to play a dominant role and many complex phase diagrams or discordant observations between sets of experiments might in fact be caused by uncontrolled rates of compressions. Unfortunately, in many experimental studies the PIR is not monitored or anyway

hardly ever reported in publications. Therefore, this crucial information may not be available to those scientists who try to reproduce previously obtained forms.

Examples of polymorphism arising from differing rates of compression of liquids have been reported recently.[39] The effect of the compression rate on the solid-state phase transitions has also been described, but for very few systems, such as pure elements [9,10,11] and ice.[5–8,40] The case study polymorphism of L-serine described in this work illustrates the importance of systematic and detailed studies of the kinetic effects in pressure-induced phase transitions in a wide range of various systems. The PIR adds a very important new perspective to PT phase diagrams normally analyzed. In particular, it may allow production of otherwise inaccessible phases. More studies on other polymorphic systems may enable in the future to elaborate models and reach more comprehensive conclusions on the role of the PIR.

ASSOCIATED CONTENT

Supporting Information. Additional figures. Equations of state and lattice parameters. Sample, DAC and data collection, data treatment and topological analysis details. Crystal structure data of L-Ser IV. This material is available free of charge via the Internet at http://pubs.acs.org.

Structural Data. A CIF file of the L-Ser IV structure is deposited at the Cambridge Crystallographic Data Centre, CCDC number 1412832.

AUTHOR INFORMATION

Corresponding Author

*Email: piero.macchi@dcb.unibe.ch

*Email: nicola.casati@psi.ch

Notes

The authors declare no competing financial interests.

ACKNOWLEDGMENT

We acknowledge support from the Swiss National Science Foundation (project 144534). M. F. thanks Dr. Alan Coelho for helpful discussions. E. B. acknowledges support from Russian National Science Foundation (project 14-13-00834) and helpful discussions with Dr. Alexander Matvienko and Dr. Stanislav Chizhik.

REFERENCES

(1) Boldyreva E. V. High-Pressure Polymorphs of Molecular Solids: When Are They Formed, and When Are They Not? Some Examples of the Role of Kinetic Control. Cryst. Growth. Des. **2007**, 7, 1662–1668. DOI: 10.1021/cg070098u

(2) Shekar N. V. C.; Rajan K. G. Kinetics of Pressure Induced Structural Phase Transitions – A Review. Bull. Mater. Sci. **2001**, 24, 1–21. DOI: 10.1007/BF02704834

(3) Perillat J. P. Kinetics of High-Pressure Mineral Phase Transformations Using In Situ Time-Resolved X-Ray Diffraction in the Paris-Edinburgh Cell: A Practical Guide for Data Acquisition and Treatment. Min. Mag. **2008**, 72, 683–695. DOI: 10.1180/minmag.2008.072.2.683

(4) Evans W. J.; Yoo C. S.; Lee G. W.; Cynn H.; Lipp M. J.; Visbeck K. Dynamic Diamond Anvil Cell (dDAC): A Novel Device for Studying the Dynamic-Pressure Properties of Materials. Rev. Sci. Instrum. **2007**, 78, 073904. DOI: 10.1063/1.2751409

(5) Lee G. W.; Evans W. J.; Yoo C. S. Crystallization of Water in a Dynamic Diamond-Anvil Cell: Evidence for Ice VII-Like Local Order in Supercompressed Water. Phys. Rev. B **2006**, 74, 134112. DOI: 10.1103/PhysRevB.74.134112

(6) Lee G. W.; Evans W. J.; Yoo C. S. Dynamic Pressure-Induced Dendritic and Shock Crystal Growth of Ice VI. P. Natl. Acad. Sci. USA **2007**, 104, 9178–9181. DOI: 10.1073/pnas.0609390104

(7) Chen J. Y.; Yoo C. S. High density amorphous ice at room temperature. P. Natl. Acad. Sci. USA **2011**, 108, 7685–7688. DOI: 10.1073/pnas.1100752108

(8) Chen J. Y.; Kim M.; Yoo C. S.; Liermann H. P.; Evans W. J. Time-Resolved X-Ray Diffraction Across Water-Ice-VI/VII Transformations Using the Dynamic-DAC. J. Phys. Conf. Ser. **2014**, 500, 142006. DOI: 10.1088/1742-6596/500/14/142006

(9) Chen J. Y.; Yoo C. S.; Evans W. J.; Liermann H. P.; Cynn H.; Kim M.; Jenei Z. Solidification and Fcc to Metastable Hcp Phase Transition in Krypton Under Variable Compression Rates. Phys. Rev. B **2014**, 90, 114104. DOI: 10.1103/PhysRevB.90.144104

(10) Haberl B.; Guthrie M.; Malone B. D.; Smith J. S.; Sinogeikin S. V.; Cohen M. L.; Williams J. S.; Shen G.; Bradby J. E. Controlled Formation of Metastable Germanium Polymorphs. Phys. Rev. B **2014**, 89, 144111. DOI: 10.1103/PhysRevB.89.144111

(11) Velisavljevic N.; Sinogeikin S.; Saavedra R.; Chellappa R. S.; Rothkirch A.; Dattelbaum D. M.; Konopkova Z.; Liermann H. P.; Bishop M.; Tsoi G.M.; et al. Time-Resolved X-Ray

Diffraction and Electrical Resistance Measurements of Structural Phase Transitions in Zirconium. J. Phys. Conf. Ser. **2014**, 500, 032020. DOI: 10.1088/1742-6596/500/3/032020

(12) Lanza A.; Fiolka C.; Fisch M.; Casati N.; Skoulatos M.; Rüegg C.; Krämer K. W.; Macchi P. New Magnetic Frameworks of $[(CuF_2(H_2O)_2)_x(pyz)]$. Chem. Comm. **2014**, 50, 14504–14507. DOI: 10.1039/c4cc06696k

(13) Boldyreva E.V. Combined X-Ray Diffraction and Raman Spectroscopy Studies of Phase Transitions in Crystalline Amino Acids at Low Temperature and High Pressure: Selected Examples. Phase Transit. **2009**, 82, 303–321. DOI: 10.1080/01411590902838656

(14) Boldyreva E. V.; Sowa H.; Ahsbahs H.; Goryainov S. V.; Chernyshev V. V.; Dmitriev V. P.; Seryotkin Y. V.; Kolesnik E. N.; Shakhshneider T. P.; Ivashevskaya S. N.; et al. Pressure-Induced Phase Transitions in Organic Molecular Crystals: A Combination of X-Ray Single-Crystal and Powder Diffraction, Raman and IR-spectroscopy. J. Phys. Conf. Ser. **2008**, 121, 022023. DOI: 10.1088/1742-6596/121/2/022023

(15) Moggach S. A. High-Pressure Polymorphism in Amino Acids. Crystallogr. Rev. **2008**, 14, 143–184. DOI: 10.1080/08893110802037945

(16) Funnell N. P.; Marshall W. G.; Parsons S. Alanine at 13.6 GPa and its Pressure-Induced Amorphisation at 15 GPa. CrystEngComm **2011**, 13, 5841–5848. DOI: 10.1039/c1ce05487b

(17) Olsen J. S.; Gerward L.; Freire P. T. C.; Mendes Filho J.; Melo F. E. A.; Souza Filho A. G. Pressure-Induced Phase Transformation in L-Alanine Crystals. J. Phys. Chem. Solids **2008**, 69, 1641–1645. DOI: 10.1016/j.jpcs.2007.12.005

(18) Tumanov N. A.; Boldyreva E. V.; Kolesov B. A.; Kurnosov A. V.; Quesada Cabrera R. Pressure-Induced Phase Transition in L-Alanine, Revisited. Acta Cryst. B **2010**, 66, 458–471. DOI: 10.1107/S010876811001983X

(19) Zakharov B. A.; Kolesov B. A.; Boldyreva E. V. Effect of Pressure on Crystalline L- and DL-Serine: Revisited by a Combined Single-Crystal X-Ray Diffraction at a Laboratory Source and Polarized Raman Spectroscopy Study. Acta Cryst. B **2012**, 68, 275–286. DOI: 10.1107/S0108768112015960

(20) Zakharov B. A.; Tumanov N. A.; Boldyreva E. V. β-Alanine Under Pressure: Towards Understanding the Nature of Phase Transitions. CrystEngComm **2015**, 17, 2074–2079. DOI: 10.1039/C4CE02550D

(21) Mnyukh, Y. Fundamentals of Solid-State Phase Transitions, Ferromagnetism and Ferroelectricity; 1st Books Library: Bloomington, IN, USA, 2002

(22) Boldyreva E.V.; Kolesnik E.N.; Drebushchack T.N.; Ahsbahs H.; Beukes J.A.; Weber H.P. A Comparative Study of the Anisotropy of Lattice Strain Induced in the Crystals of L-Serine by Cooling Down to 100 K or by Increasing Pressure up to 4.4 GPa. Z. Kristallogr. **2005**, 220, 58–65. DOI: 10.1007/s10634-005-0052-1

(23) Drebushchak T. N.; Sowa H.; Seryotkin Y. V.; Boldyreva E. V.; Ahsbahs H. L-Serine III at 8.0 GPa. Acta Cryst. E **2006**, 62, 0452–0454. DOI: 10.1107/S1600536806032508

(24) Moggach S. A.; Allan D. R.; Morrison C. A.; Parsons S.; Sawyer L. Effect of Pressure on the Crystal Structure of L-Serine-I and the Crystal Structure of L-Serine-II at 5.4 GPa. Acta Cryst. B **2005**, 61, 58–68. DOI: 10.1107/S0108768104031787

(25) Boldyreva E. V.; Sowa H.; Seryotkin Y. V.; Drebushchack T. N.; Ahsbahs H.; Chernyshev V.; Dmitriev V. Pressure-Induced Phase Transitions in Crystalline L-Serine Studied by Single-Crystal and High-Resolution Powder X-Ray Diffraction. Chem. Phys. Lett. **2006**, 429, 474–478. DOI: 10.1016/j.cplett.2006.08.092

(26) Moggach S. A.; Marshall W. G.; Parsons S. High-Pressure Neutron Diffraction Study of L-Ser-I and L-Ser-II, and the Structure of L-Ser-III at 8.1 GPa. Acta Cryst. B **2006**, 62, 815–825. DOI: 10.1107/S010876810601799X

(27) Wood P. A.; Francis D.; Marshall W. G.; Moggach S. A.; Parsons S.; Pidcock E.; Rohl A. L. A Study of the High-Pressure Polymorphs of L-Serine Using Ab Initio Structures and PIXEL Calculations. CrystEngComm **2008**, 10, 1154–1166. DOI: 10.1039/b801571f

(28) Klotz S.; Chervin J. C.; Munsch P.; Le Marchand G. Hydrostatic Limits of 11 Pressure Transmitting Media. J. Phys. D. Appl. Phys. **2009**, 42, 075413. DOI: 10.1088/0022-3727/42/7/075413

(29) Angel R.J.; Allan D.R.; Miletich R.; Finger W. The Use of Quartz as an Internal Pressure Standard in High-Pressure Crystallography. J. Appl. Cryst. **1997**, 30, 461–466. DOI: 10.1107/S0021889897000861

(30) Syassen K. Ruby Under Pressure. High Pressure Res. **2008**, 28, 75–126. DOI: 10.1080/0895795080223564

(31) Willmott P. R.; Meister D.; Leake S. J.; Lange M.; Bergamaschi A.; Böge M.; Calvi M.; Cancellieri C.; Casati N.; Cervellino A.; et al. The Materials Science Beamline Upgrade at the

Swiss Light Source. J. Synchrotron Radiat. **2013**, 20, 667–682. DOI: 10.1107/S0909049513018475

(32) Coelho A.A. TOPAS-Academic V5. Coelho Software, Brisbane, **2012**

(33) Stinton G. W.; Evans J. S. O. Parametric Rietveld Refinement. J. Appl. Cryst. **2007**, 40, 87–95. DOI: 10.1107/S0021889806043275

(34) Coelho A.A. Structure Solution by Simulated Annealing. J. Appl. Cryst. **2000**, 33, 899–908. DOI: 10.1107/S002188980000248X

(35) Dovesi R.; Saunders V. R.; Roetti C.; Orlando R.; Zicovich-Wilson C. M.; Pascale F.; Civalleri B.; Doll K.; Harrison N. M.; Bush I. J.; D'Arco P.; Llunell M. CRYSTAL09 User's Manual. University of Torino, Torino, **2009**

(36) Blatov A. P.; Shevchenko A.P; Proserpio D. M. Applied Topological Analysis of Crystal Structures with the Program Package ToposPro. Cryst. Growth. Des. **2014**, 14, 3576-3586. DOI: 10.1021/cg500498k

(37) Rosi N. L.; Kim J.; Eddaoudi M.; Chen B.; O'Keefe M.M Yaghi O. M. Rod Packings and Metal−Organic Frameworks Constructed from Rod-Shaped Secondary Building Units. J. Am. Chem. Soc. **2005**, 127(5), 1504-1518. DOI: 10.1021/ja045123o

(38) O'Keefe M. Sphere Packings and Space Filling by Congruent Simple Polyhedra. Acta Cryst. A **1998**, 54, 320-329. DOI: 10.1107/S0108767397017893

(39) Ridout, J.; Price, L. S.; Howard, J. A. K.; Probert, M. R. Cryst. Growth & Des., **2014**, 14, 3384–3391, DOI: 10.1021/cg500331u

(40) Bauer, M.; Elsaesser, M. S.; Winkel, K.; Mayer, E.; Loerting, T. Phys. Rev. B., **2008**, *77*, 220105. DOI 10.1103/PhysRevB.77.220105

TOC GRAPHICS